Experimental study of high-energy fission and quasi-fission with fusion-induced fission reactions at VAMOS++

D. Fernández[1,*], *M. Caamaño*[1,**], *D. Ramos*[2,***], *A. Lemasson*[2], *M. Rejmund*[2], *H. Álvarez-Pol*[1], *L. Audouin*[3], *J. D. Frankland*[2], *B. Fernández-Domínguez*[1], *E. Galiana-Baldó*[4], *J. Piot*[2], *C. Schmitt*[5], *D. Ackermann*[2], *S. Biswas*[2], *E. Clement*[2], *D. Durand*[6], *F. Farget*[6], *M. O. Fregeau*[2], *D. Galaviz*[4], *A. Heinz*[7], *A. Henriques*[8], *B. Jacquot*[2], *B. Jurado*[8], *Y. H. Kim*[2], *P. Morfouace*[2], *D. Ralet*[9], *T. Roger*[2], *P. Teubig*[4], and *I. Tsekhanovich*[8]

[1]IGFAE – Universidad de Santiago de Compostela, E–15706 Santiago de Compostela, Spain
[2]GANIL, CEA/DRF-CNRS/IN2P3, BP 55027, F-14076 Caen Cedex 5, France
[3]IPN Orsay, Université de Paris-Saclay, CNRS/IN2P3, F-91406 Orsay Cedex, France
[4]LIP Lisboa, 1649-003 Lisbon, Portugal
[5]IPHC Strasbourg, Université de Strasbourg-CNRS/IN2P3, F-67037 Strasbourg Cedex 2, France
[6]LPC Caen, Université de Caen Basse-Normandie-ENSICAEN-CNRS/IN2P3, F-14050 Caen Cedex, France
[7]Department of Physics, Chalmers University of Technology, SE-41296 Göteborg, Sweden
[8]CENBG, IN2P3/CNRS-Université de Bordeaux, F-33175 Gradignan Cedex, France
[9]CSNSM, CNRS/IN2P3, Université de Paris-Saclay, F-91405 Orsay, France

Abstract. Over the past decade, inverse kinematics has been increasingly employed in experimental studies of fission. This approach has yielded a wealth of new observables that can be obtained in single measurements, enabling their analysis and correlations. One ongoing application of this technique involves a series of experiments performed at GANIL using the variable-mode, large-acceptance VAMOS++ spectrometer. A recent experiment focused on examining the survival of nuclear structure effects at high excitation energy in both fission and quasi-fission. The results of the study involved a full isotopic identification of fragments, as well as an analysis of the elemental yields their relation to fission dynamics. The results indicate that fission and quasi-fission involve different mechanisms, which could be exploited to distinguish between the two phenomena.

1 Introduction

Although both fission and quasi-fission lead to similar final products, there are notable distinctions between these processes. Firstly, fission comes from an equilibrated compound nucleus, while quasi-fission does not. Additionally, quasi-fission is significantly faster than fission [1]. Researchers aim to identify observables that can differentiate between the two phenomena, and the complete identification of fragments offers new opportunities.

A prior experiment [2] demonstrated that in fusion-induced fission of ^{250}Cf, structural effects may persist in both the neutron-to-proton ratio of fragments and the total kinetic energy, even at high excitation energies of approximately 40 MeV.

In 2017, the E753 experiment was performed at GANIL using the VAMOS++ spectrometer to study the fission and quasi-fission processes also at high excitation energy, and analyse the survival of nuclear structure effects in both processes. The study of fusion-fission reactions is critical for advancing our knowledge of nuclear physics and has important practical applications such as nuclear energy production and nuclear waste management. In this paper, preliminary results of ^{265}Db high-energy fission from ^{238}U + ^{27}Al reaction are presented and discussed. The isotopic-fission yields $Y(Z, A)$, the elemental yields $Y(Z)$, the neutron excess and the velocity in center of mass are presented.

2 Experimental setup

VAMOS++ is a variable mode spectrometer [3, 4] composed of a large magnetic dipole and two quadrupoles, and a set of detectors at the focal plane that measure the energy, energy loss, angles and positions before and after the magnets, and time of flight of those particles that reach the end of the focal plane. The magnetic rigidity is reconstructed using the positions and the angles at focal plane, while the emission vector is measured with those at the target position, before the spectrometer. Regarding the fission fragments, the measured observables are: atomic number (Z), mass number (A), and velocity vector. For the fissioning system, Z, A, and its excitation energy (E^*) are obtained [5].

The VAMOS++ angular acceptance is $\Delta\theta$=±7° and $\Delta\phi$=±10°. In this experiment, the spectrometer was used in two settings of central magnetic rigidity ($B\rho_0$) and an-

*e-mail: dani.fernandez@usc.es
**e-mail: manuel.fresco@usc.es
***e-mail: diego.ramos@ganil.fr

gle ($\theta_{\rm lab}$): $B\rho_0$=1.24 Tm, $\theta_{\rm lab}$=14°; and $B\rho_0$=1.1 Tm, $\theta_{\rm lab}$ = 21.5°. Further details on VAMOS++ along with typical performances for fission-fragment detection are given in Refs. [6–8].

In this experiment, a ^{238}U beam at 5.9A MeV impinged on four different light targets (0.5 mg/cm^2 of ^{9}Be, 0.1 mg/cm^2 of $^{\rm nat}$B, 0.5 mg/cm^2 of ^{24}Mg, and 0.2 mg/cm^2 of ^{27}Al) to generate different fissioning systems (FS) through transfer and fusion reactions. In the case of transfer or inelastic reactions, the target-like recoil is measured with a silicon telescope placed around the target. Fusion reactions are assumed when no recoil is detected [9]. Once a FS is formed, it splits into two fission fragments (FF) and one of them may be detected in VAMOS++.

Using inverse kinematics in fission experiments offers several advantages. One of the key benefits is the higher velocity of the FF in the laboratory frame, which facilitates their traversal of multiple detector layers. This, in turn, provides access to a broader range of observables that cannot be achieved through direct kinematics. Additionally, inverse kinematics allows for better control over the reaction products, leading to more accurate measurements and increased understanding of the fission process. Finally, the use of inverse kinematics can also reduce the effects of background noise, which can improve the overall quality of the experimental results.

3 Results with the aluminium target

The compound nucleus produced in the reaction with the Al target is ^{265}Db with $E^* = 61.2$ MeV. The properties of this compound and its subsequent fission products provide valuable insights into the fundamental physics of nuclear fusion and fission reactions.

3.1 Fission yields

Isotopic-fission yields are derived using the procedure presented in Refs. [10, 11]. In this procedure, the fission events are counted and weighted by various factors, including the spectrometer acceptance, the angular and intrinsic efficiencies, and the relative normalisation between settings. The procedure also includes the subtraction of contamination from transfer-fission events. The resulting isotopic-fission yields provide information about the distribution of fission products and can be used to study the underlying process.

Figure 1 displays the isotopic yields of ^{265}Db as a function of the fragment mass, with each color representing a different atomic number (Z) between $Z = 30$ and $Z = 66$. In this and the rest of the figures of this document, the error bars represent the statistical uncertainties; systematic uncertainties range from 2% in the heavier fragments up to 10% in the lighter ones. The resolution in the identification of atomic number is $\Delta Z/Z \sim 1/80$, while the resolution in mass identification is $\Delta A/A \sim 1/200$.

The elemental yields $Y(Z)$ can be calculated by summing the contributions of each mass A: $Y(Z) = \sum_A Y(Z, A)$. The resulting elemental yields are displayed

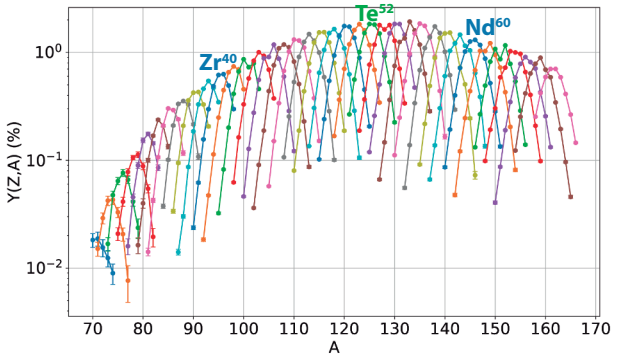

Figure 1. Isotopic fission yields $Y(Z, A)$ of fusion-induced fission of ^{265}Db at $E^* = 61.2$ MeV. Each colour line corresponds to one element. Zr^{40}, Te^{52}, and Nd^{60} are shown for reference.

in Fig. 2 and are compared to the predictions of the semi-empirical code GEF [12] as well as a previous measurement of a similar reaction [13]. In addition, an approximation of the quasi-fission distribution is shown in a solid red line, which is obtained from the difference between the yield and its complementary using the symmetry of the elemental fission yields. This approximation assumes that the yield for a given element $Y(Z)$ is equal to the yield of its complementary element at $Z_{comp} = Z_{FS} - Z$, where Z_{FS} is the nuclear charge of the compound nucleus.

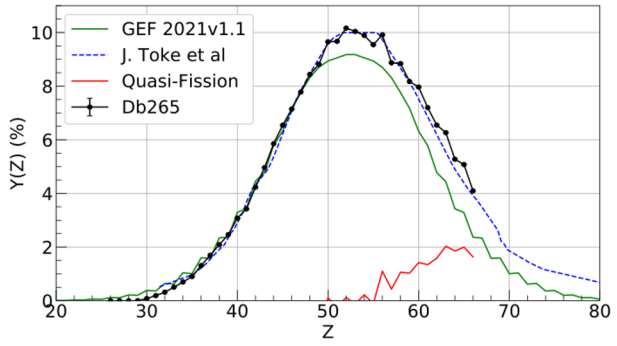

Figure 2. Elemental yield distribution $Y(Z)$ of fragments from ^{265}Db fusion-fission reactions (black points and solid black line) compared with the GEF prediction (solid green line) and previous measurement from [13] (dashed blue line). The minimum quasi-fission contribution is shown with solid red line.

The results reveal a non-symmetric distribution, which is produced by to the restricted coverage of the centre-of-mass (c.m.) angle of the experiment. This limited coverage is illustrated in Fig. 3, where the blue solid lines indicate the angle restriction, and the dashed blue lines shows the limits of mass identification (before neutron evaporation). As mentioned earlier, there is a strong correlation between the fragment mass and the c.m. angle. In this case, the experimental coverage only includes the heavy-fragment mass of quasi-fission, represented by the solid red line circle in Fig. 3, while the corresponding light fragments would be in the complementary c.m. angle, indicated by the dashed red line circle, which is not covered in this experiment.

The $Y(Z)$ distribution is in agreement with the previous measurement [13], once the same restrictions are applied. The comparison with the GEF model [12] shows an agreement on the light-fragment part of the distribution. This is because the fission component of the reaction is not affected by the restriction in angular coverage.

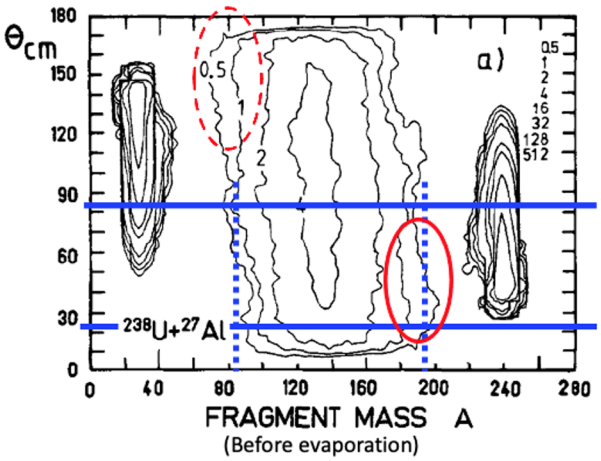

Figure 3. Experimental measurement [13] of fragment masses before evaporation versus c.m. angle for the reaction ^{238}U + ^{27}Al with the VAMOS++ limits in angle and mass (blue solid and dashed lines, respectively). Red circles show approximately the quasi-fission contribution to the reaction. The solid red line corresponds to the contribution accessible with VAMOS++.

3.2 Neutron excess

The fissioning system is excited before the saddle point and will emit neutrons. Since the information on these neutrons cannot be accessed directly in this experiment, an estimation with the GEF code is used, resulting in a FS average mass of $\langle A_{\mathrm{FS}}\rangle$~262.4. Assuming a negligible proton emission, the pre-evaporation masses of the fragments $\langle A_i^*\rangle$ can be evaluated with this estimated mass $\langle A_{\mathrm{FS}}\rangle$. The nuclear structure effects would appear in the pre-evaporation step (at scission). The information about the fissioning system at the scission point can be obtained from the neutron excess after evaporation and the fragment velocities in c.m. The neutron excess $\langle N\rangle/Z = [(\sum_A A \cdot Y(Z,A))/(\sum_A Y(Z,A)) - Z]/Z$ is shown in Fig. 4 compared to GEF.

Since the fissioning system is highly excited, it can emit neutrons before reaching the saddle point, leading to a decrease in the effective excitation energy before the start of the fission process. The calculations with GEF show a smaller $\langle N\rangle/Z$ than what is measured; although the evolution as a function of Z is very similar. GEF predicts a large number of emitted neutrons before scission, including 2.4 pre-saddle neutrons, which could explain the excess. However, there is no way to access information on these neutrons due to current experimental limitations. Further studies on neutron evaporation are necessary to explain this behaviour.

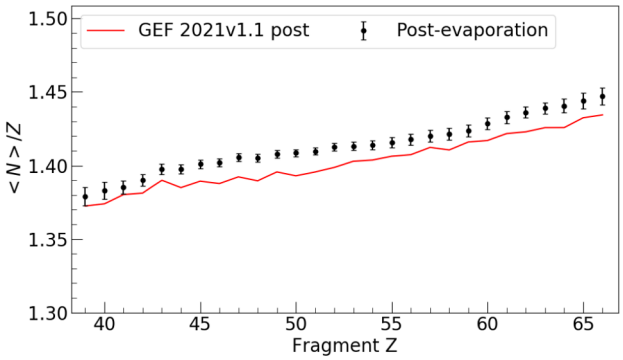

Figure 4. Post-evaporation average neutron-excess $\langle N\rangle/Z$ of ^{265}Db fission fragments as a function of fragment Z (black symbols) and corresponding GEF predictions (solid red line).

3.3 Isotopic velocities

As both the laboratory frame (V_{lab}, θ_{lab}) and the fissioning system frame are measured, the c.m. velocity of the fission fragments $V_{\mathrm{c.m.}}^{\mathrm{FF}}$ can be determined on an event-by-event basis, enabling access to fission dynamics. Figure 5 displays $V_{\mathrm{c.m.}}^{\mathrm{FF}}$ as a function of the fragment A with each panel corresponding to one Z. Although the experimental data agree well with GEF for $Z > 40$, there is a deviation observed for the light fragments. The figure exhibits a slight overestimation in GEF prediction, with the largest deviations occurring in more neutron-rich isotopes.

4 Conclusions

The preliminary results presented were obtained with the VAMOS++ setup, which allows for the measurement of a variety of observables, including complete isotopic and elemental yield distributions of the ^{265}Db fissioning system. The data analysis reveals a contribution from the quasi-fission process in the elemental fission yields, which is identified with the heaviest contribution of the quasi-fission. This process can contribute to the observed fragment mass distributions, and it is important to account for it when studying heavy-ion reactions. Furthermore, the neutron excess and isotopic velocity in the centre-of-mass frame of the fission fragments are also reported.

References

[1] D. J. Hinde, R. du Rietz, C. Simenel, M. Dasgupta, A. Wakhle, M. Evers, and D. H. Luong, AIP Conf. Proc. 1423, 65 (2012).

[2] M. Caamaño, F. Farget, O. Delaune, K. H. Schmidt, C. Schmitt, L. Audouin, C. O. Bacri, J. Benlliure, E. Casarejos, X. Derkx, B. Fernández-Domínguez, L. Gaudefroy, C. Golabek, B. Jurado, A. Lemasson, D. Ramos, C. Rodríguez-Tajes, T. Roger, and A. Shrivastava. Phys. Rev. C 92, 034606 (2015).

[3] S. Pullanhiotan, M. Rejmund, A. Navin, W. Mittig, S. Bhattacharyya, Nucl. Instr. and Meth. A 593, 343 (2008).

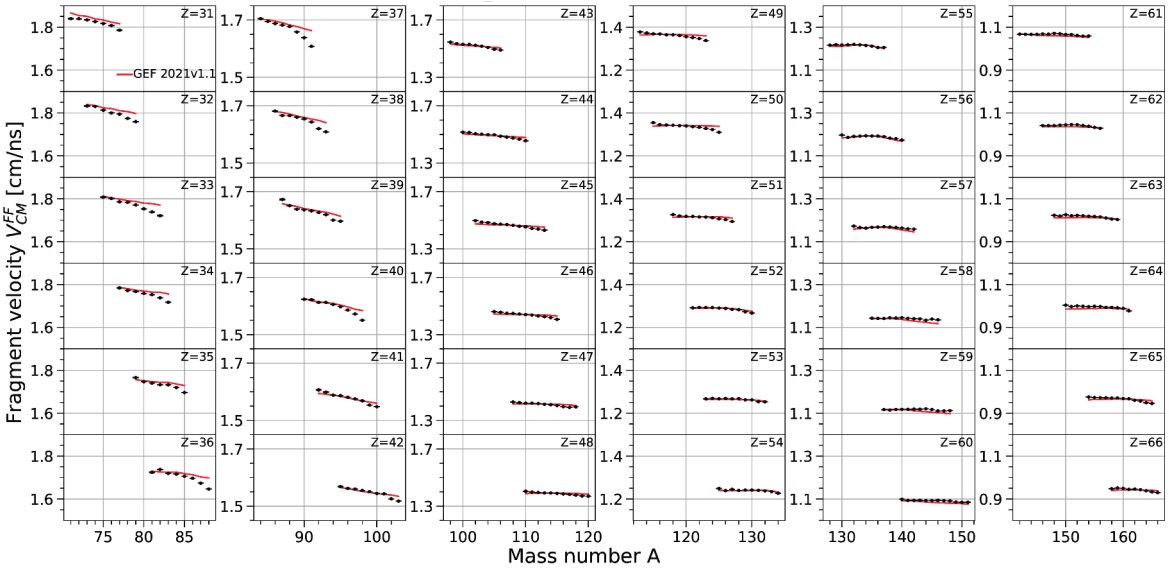

Figure 5. Each panel shows the centre of mass velocity as a function of A for the different elements produced in fusion-fission of ^{265}Db (black points). The GEF prediction is shown with red lines.

[4] M. Rejmund, B. Lecornu, A. Navin, C. Schmitt, S. Damoy, O. Delaune, J.M. Enguerrand, G. Fremont, P. Gangnant, L. Gaudefroy, et al., Nucl. Instr. and Meth. A 646, 184 (2008).

[5] C. Rodríguez-Tajes, F. Farget, X. Derkx, M. Caamaño, O. Delaune, K.-H. Schmidt, E. Clement, A. Dijon, A. Heinz, T. Roger, L. Audouin, J. Benlliure et al., Phys. Rev. C 89, 024614 (2014).

[6] M. Rejmund, B. Lecornu, A. Navin, C. Schmitt, S. Damoy, O. Delaune, J.M. Enguerrand, G. Fremont, P. Gangnant, L. Gaudefroy, B. Jacquot, J. Pancin et al., Nucl. Instr. and Meth. A 646, 184 (2011).

[7] M. Vandebrouck, A. Lemasson, M. Rejmund, G. Fremont, J. Pancin, A. Navin, C. Michelagnoli, J. Goupil, C. Spitaels, and B. Jacquot. Nucl. Instr. and Meth. A 812,112 (2016).

[8] Y. Kim, A. Lemasson, M. Rejmund, A. Navin, S. Biswas, C. Michelagnoli, I. Stefan, R. Banik, P. Bednarczyk, S. Bhattacharya, S. Bhattacharyya, E. Clement et al., Eur. Phys. J. A 53, 162 (2017).

[9] D. Ramos, M. Caamaño, A. Lemasson, M. Rejmund, L. Audouin, H. Álvarez-Pol, J. D. Frankland, B. Fernández-Domínguez, E. Galiana-Baldó, J. Piot, D. Ackermann, S. Biswas, E. Clement, D. Durand, F. Farget, M. O. Fregeau, D. Galaviz, A. Heinz, A. I. Henriques, B. Jacquot, B. Jurado, Y. H. Kim, P. Morfouace, D. Ralet, T. Roger, C. Schmitt, P. Teubig, and I. Tsekhanovich, Phys. Rev. L 123, 092503 (2019).

[10] M. Caamaño, O. Delaune, F. Farget, X. Derkx, K.-H. Schmidt, L. Audouin, C.-O. Bacri, G. Barreau, J. Benlliure, E. Casarejos, A. Chbihi, B. Fernández-Domínguez et al., Phys. Rev. C 88, 024605 (2013).

[11] D. Ramos, M. Caamaño, F. Farget, C. Rodríguez-Tajes, L. Audouin, J. Benlliure, E. Casarejos, E. Clement, D. Cortina, O. Delaune, X. Derkx, A. Dijon et al., Phys. Rev. C 97, 054612 (2018).

[12] K.-H. Schmidt, B. Jurado, C. Amouroux, and C. Schmitt, Nucl. Data Sheets 131, 107 (2016).

[13] J. Toke, R. Bock, G. X. Dai, A. Gobbi, S. Gralla, K. D. Hildenbrand, J. Kuzminski, W. F. J. Müller, A. Olmi, and H. Stelzer Nucl. Phys. A 440, 327 (1985).